

# Behavioral Modeling of Polycrystalline Module ET-P660230WW

George Angelov<sup>1)</sup>, Rostislav Rusev<sup>2)</sup>, Anna Andonova<sup>1)</sup>, Marin Hristov<sup>1)</sup>

<sup>1)</sup>Dept. of Microelectronics, FETT, ECAD Lab, Technical University of Sofia, Bulgaria

<sup>2)</sup>Dept. of Techn. Mngt. Comm. Systems, FTK, ECAD Lab, Technical University of Sofia, Bulgaria

gva@ecad.tu-sofia.bg

**Abstract:** A behavioral model of polycrystalline solar module ET-P660230WW applying semi-empirical approach is presented. The model equations are coded in Matlab. The simulation results are verified against the data provided in the data sheet of the module.

## 1. INTRODUCTION

World demand for energy is forecasted to double by 2050 and to triple by 2100. Incremental improvements in existing energy networks will not be adequate to supply this demand in a sustainable way. Finding sufficient supplies of clean energy for the future is becoming a global issue.

Renewable energy sources are prospective area for efficient and environmental mass energy production. Photovoltaics (PV) are already well recognized as efficient renewable energy source as they are converting light (photons) to electricity (voltage). Given the enormous potential of solar energy, photovoltaics may well become a major source of clean electricity in the future. However, for this to happen, the electricity generation costs for PV systems need to be reduced and the efficiency of converting sunlight into electricity needs to increase.

## 2. SOLAR CELL MODEL

Correct simulation results in the PV design process when using system level design tools are obtained when developing high level models of the solar cells that can be used with the other electrical models in the electric circuits simulations.

### 2.1. Modeling Approach

Analog and mixed digital-analog hardware description languages (HDLs) allow for creating models of analog and mixed signal circuits at high level of abstraction by defining electrical equations

for the nodes and branches. They can be used to create models of elements or entire system using differential and algebraic equations (DAE). These models are defined in order to describe the device electrical characteristics and to be used in commercial CAD tools such as Cadence, Synopsys, mentor graphics, etc.

To ensure correct simulation results in the PV design process when using system level design tools, it is very important to have high level models of solar cells that can be used in concert with the other electrical models in the simulated electrical circuits.

At the stage of model optimization, the general-purpose Matlab environment might be used for simulation of model equations. The high speed calculation in Matlab is also quite useful for extraction and optimization of model parameters.

In this paper, we present a simplified behavioral model of state-of-the-art commercial PV module operating in real conditions. The model consists of semi-empirical equations coded in Matlab. The results are compared to data given in the product data sheet.

### 2.2. Model Formulation

The solar cell model is presented in Fig. 1. The inputs of the solar cell are the solar irradiation ( $G$ ) and the ambient temperature ( $T_a$ ). The outputs are the short circuit current ( $I_{sc}$ ), open circuit voltage ( $V_{oc}$ ), power at maximum power point (MPP) ( $P_m$ ), cell temperature ( $T_{cell}$ ), current at MPP ( $I_m$ ), voltage at MPP ( $V_m$ ).

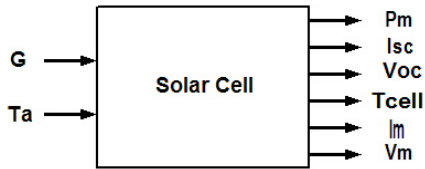


**Fig. 1.** Block diagram of solar cell in Matlab.

The behavioral model equations are semi-empirical. The short-circuit current and the open circuit voltage are derived from [7]. Below we list them in the syntax used in Matlab [8] and [9].

$$I_{SC} = (J_{SCR} * A * G / 1000) + DIFJscT * (Ta - Tr) \quad (1)$$

where  $J_{SCR}$  – current density,  $A$  – area of the module,  $DIFJscT$  – temperature coefficient of short circuit current,  $Tr$  – reference temperature.

$$T_{cell} = ((NOCT - 20) * G / 800) + Ta \quad (2)$$

where  $NOCT$  – nominal operating conditions temperature.

For  $V_{OC}$  the equations are as follows:

$$V_{OCC} = \log((I_{SC}) / (I_{SCR})) \quad (3)$$

$$V_{OC} = V_{Ocr} + V_{OCC} * (V_t * (Ta + 273)) \quad (4)$$

$V_t$  – thermal potential;  $V_t$  is calculated at the cell temperature  $T_{cell}$ .

The  $v_o$  parameter below is the normalized value of the open circuit voltage to the thermal potential  $V_t$ :

$$FF_O = (v_o - \log(v_o + 0.72)) / (1 + v_o) \quad (5)$$

The series resistance  $R_s$  can be calculated from the fill factor:

$$R_{SS} = (V_{Ocr} / I_{SCR}) \quad (6)$$

$$r_s\_znam = I_{SCR}^2 \quad (7)$$

$$R_s = R_{SS} - (P_{mr} / (FF_O * r_s\_znam)) \quad (8)$$

The current at MPP is calculated in the same manner as  $I_{SC}$ :

$$I_m = I_{mr} * (G / Gr) + DIFJscT * (Ta - Tr) \quad (9)$$

For the voltage at MPP is used

$$V_{mr} = \log(I_m / (I_{mr})) \quad (10)$$

$$V_m = V_{mr} + V_{mr} * (V_t * (T_{cell} + 273)) \quad (11)$$

From here, we obtain for fill factor – FF:

$$F_m = V_m * I_m \quad (12)$$

$$F_{SOC} = V_{OC} * I_{SC} \quad (13)$$

$$FF = F_m / F_{SOC} \quad (14)$$

Finally the maximum output power  $P_m$  is

$$P_m = V_m * I_m \quad (15)$$

### 2.3. Reference Data

The reference data against which the simulation results are verified are taken from the ET-P660230WW 230W solar cell module data sheet [6]. The module is chosen as typical product for commercial use.

## 3. SIMULATIONS

Simulations of the output current and voltage versus incident radiation on the solar cell surface at constant ambient temperature are performed in Matlab. The reference data for the solar cell are taken from solar cells' product data sheet [6]. The area of the experimental cell is  $1 \text{ cm}^2$ .

The radiation intensity is varied from  $300 \text{ W/m}^2$  to  $1000 \text{ W/m}^2$ . Fig. 2 shows the short-circuit current  $I_{SC}$  as a function of radiation intensity of the incident light at  $298 \text{ K}$ . The short-circuit current increases with the radiation intensity [6]. The behavior is close to linear in the given radiation interval (and this is confirmed in simulations, cf. Fig. 3). Almost identical to  $I_{SC}$  is the line representing maximum power point (MPP)  $P_{max}$ .

Fig. 2 also plots the dependence of the  $V_{OC}$  on radiation intensity at  $298 \text{ K}$ . It can be seen that  $V_{OC}$  increases between  $300$  to  $700 \text{ W/m}^2$  and it saturates above  $700 \text{ W/m}^2$ .

The values of  $I_{SC}$ ,  $V_{OC}$  and  $P_{max}$  on Fig. 2 are in percent because they are given as ratio between the magnitude at given irradiance divided to the value at irradiance at  $1000 \text{ W/m}^2$ .

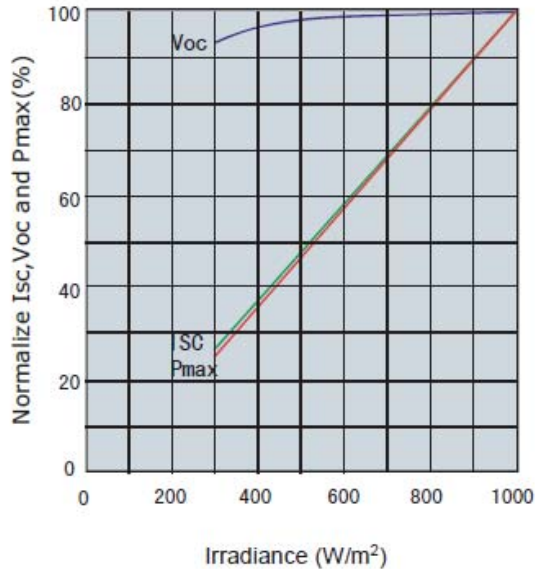


**Fig. 2.** Irradiance dependence of  $I_{SC}$ ,  $V_{OC}$  and  $P_{max}$  at temperature of 298 K.

These three characteristics are simulated by our model. First we give the simulation of the short-circuit current  $I_{SC}$  as a function of radiation intensity of the incident light at 298 K (Fig. 3).

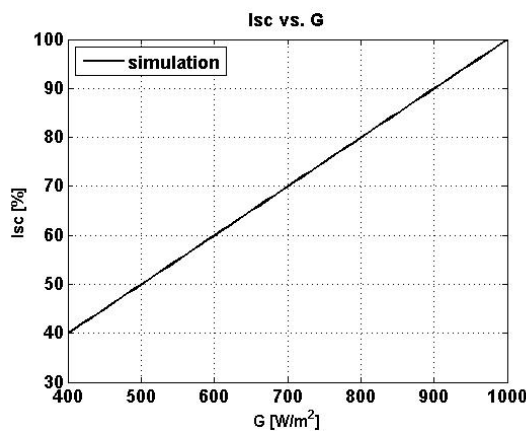


**Fig. 3.** Simulation of short-circuit current  $I_{SC}$ , as a function of radiation intensity at 298 K.

For calculation of the simulation accuracy we have compared the reference data to the simulation results of  $I_{SC}$  at radiation intensities of 400 W/m<sup>2</sup>, 600 W/m<sup>2</sup>, 800 W/m<sup>2</sup>, and 1000 W/m<sup>2</sup> – Fig. 4 and Fig. 5.

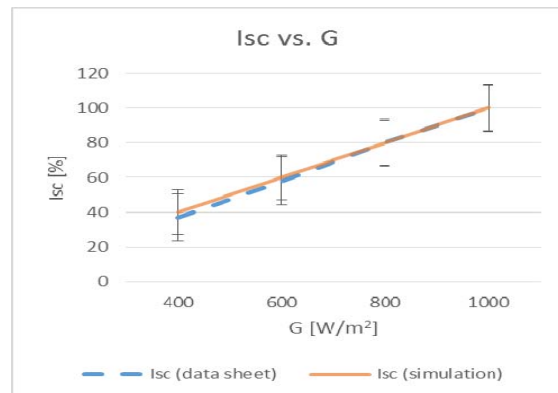


**Fig. 4.** Comparison of reference data vs. simulation of short-circuit current  $I_{SC}$  as a function of radiation intensity at temperature of 298 K.

The average accuracy is 1.25 % (Fig. 5).

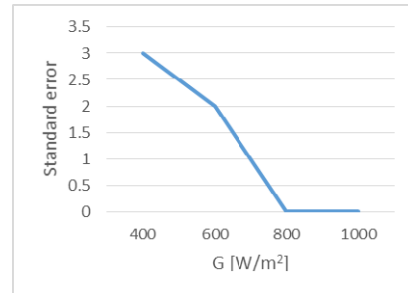


**Fig. 5.** Accuracy of simulation of the dependence of short-circuit current  $I_{SC}$  versus radiation intensity at of 298 K; average accuracy: 1.25 %.

Next, we are giving the simulation results for open-circuit voltage  $V_{OC}$  as a function of radiation intensity of the incident light at 298 K (Fig. 6).

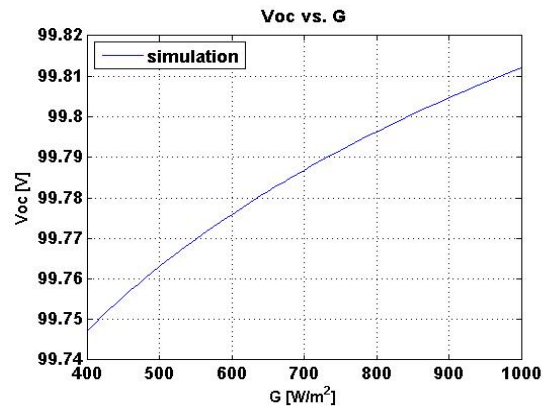


**Fig. 6.** Simulation of open-circuit voltage  $V_{OC}$  as a function of radiation intensity at 298 K.

The accuracy of simulation is again calculated by comparing the reference data to the simulation results of  $V_{OC}$  at radiation intensities of  $400 \text{ W/m}^2$ ,  $600 \text{ W/m}^2$ ,  $800 \text{ W/m}^2$ , and  $1000 \text{ W/m}^2$  – Fig. 7 and Fig. 8.

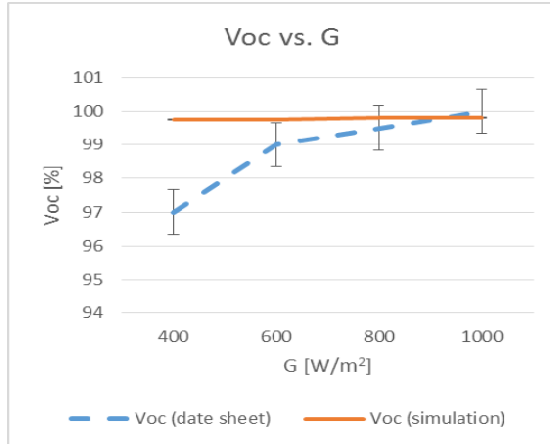


**Fig. 7.** Comparison of reference data vs. simulation of open-circuit voltage  $V_{OC}$  as a function of radiation intensity at temperature of 298 K.

The average accuracy is 1.01 % (Fig. 8).

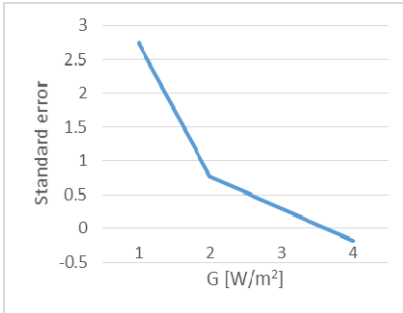


**Fig. 8.** Accuracy of simulation of the dependence of open-circuit voltage  $V_{OC}$  versus radiation intensity at of 298 K; average accuracy: 1.005 %.

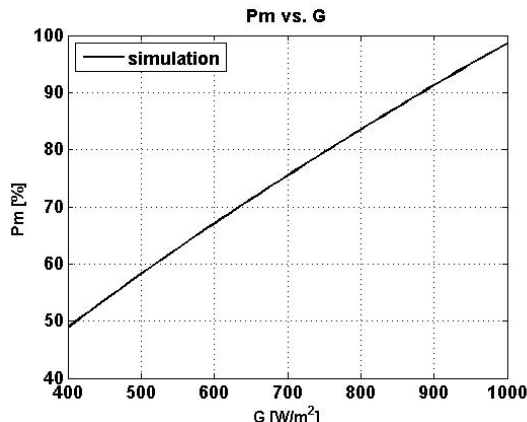


**Fig. 9.** Simulation of maximum power point (MPP)  $P_{max}$  as a function of radiation intensity at temperature of 298 K.

Below we show the simulation results for maximum power point (MPP)  $P_{max}$  as a function of radiation intensity of the incident light at 298 K (Fig. 9).

Simulation accuracy is calculated by comparing the reference data to the simulation results of  $V_{OC}$  at radiation intensities of  $400 \text{ W/m}^2$ ,  $600 \text{ W/m}^2$ ,  $800 \text{ W/m}^2$ , and  $1000 \text{ W/m}^2$  – Fig. 10 and Fig. 11.

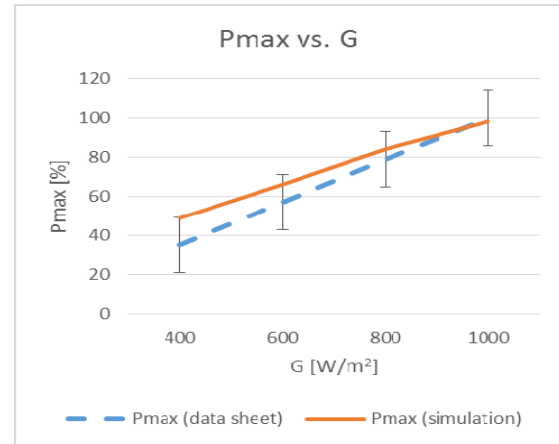


**Fig. 10.** Comparison of reference data vs. simulation of maximum power point (MPP)  $P_{max}$  as a function of radiation intensity at temperature of 298 K.

The average accuracy is 7.50 % (Fig. 11).

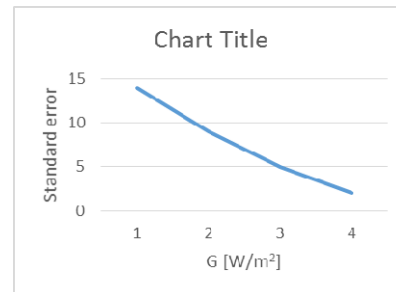


**Fig. 11.** Accuracy of simulation of the dependence of maximum power point (MPP)  $P_{max}$  versus radiation intensity at of 298 K; average accuracy: 7.5 %.

From Figures 5, 8 and 11 it is observed that is getting better with the increase of irradiation  $G$ .

In Fig. 12 we give the data sheet curves (reference data) of temperature dependence of  $I_{SC}$ ,  $V_{OC}$ , and  $P_{max}$  from the cell temperature.

In Fig. 13 is given the dependence of  $I_{SC}$  vs.  $T_{cell}$ .

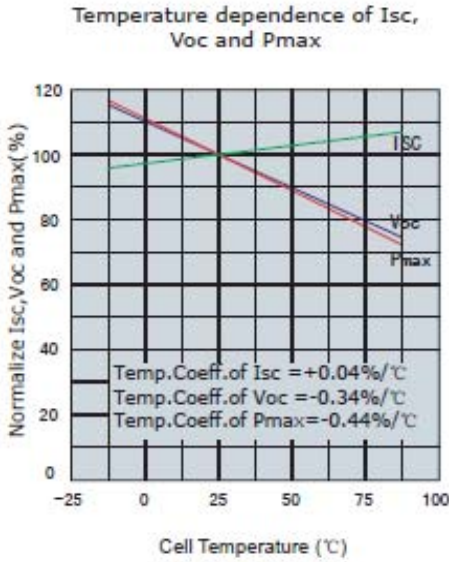


**Fig. 12.** Cell temperature dependence of  $I_{SC}$ ,  $V_{OC}$  and  $P_{max}$ .

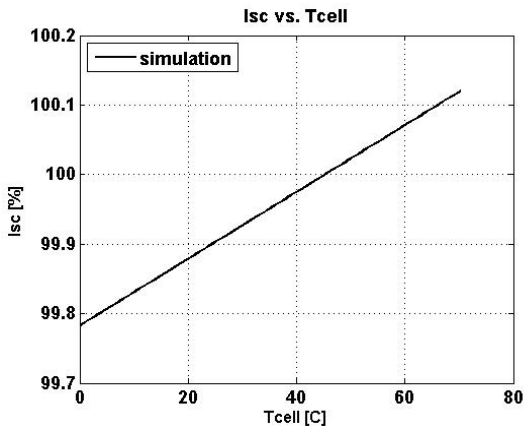


**Fig. 13.** Simulation of short-circuit current  $I_{SC}$ , as a function of cell temperature.

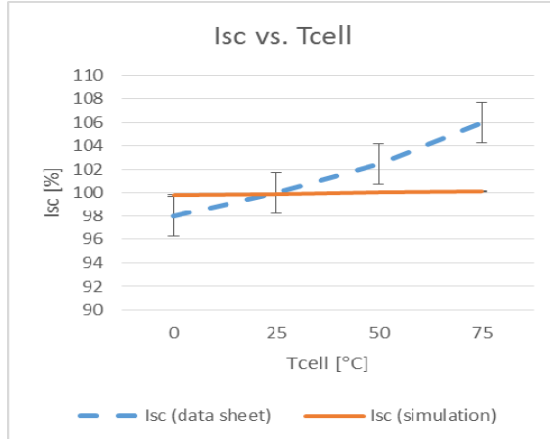


**Fig. 14.** Comparison of reference data vs. simulation of short-circuit current  $I_{SC}$  as a function of cell temperature.

Simulation accuracy is calculated by comparing the reference data to the simulation results of  $I_{SC}$  at cell temperatures of 0 °C, 25 °C, 50 °C, and 75 °C.

The average accuracy is 2.37 % (Fig. 15).

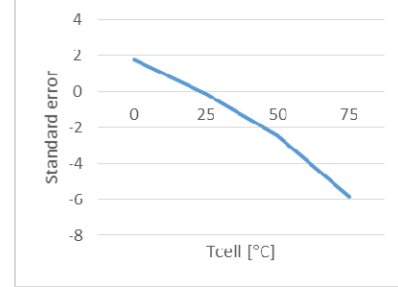


**Fig. 15.** Accuracy of simulation of the dependence of short-circuit current  $I_{SC}$  versus cell temperature; average accuracy: 2.37 %.

In Fig. 16 is the dependence of  $V_{OC}$  vs.  $T_{cell}$ .

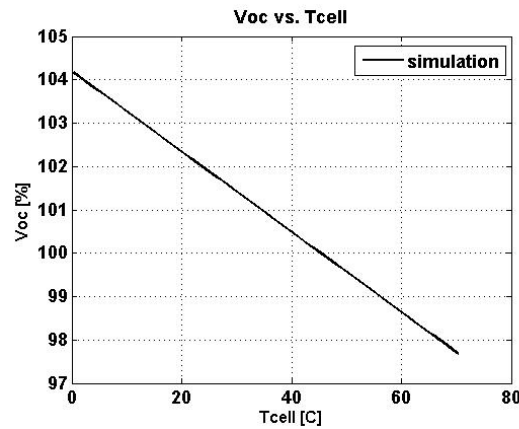


**Fig. 16.** Simulation of open-circuit voltage  $V_{OC}$ , as a function of cell temperature.

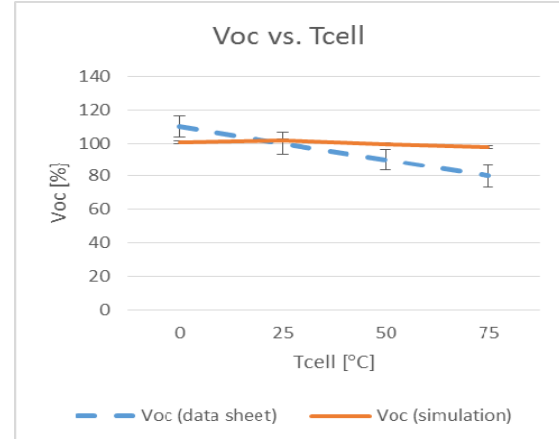


**Fig. 17.** Comparison of reference data vs. simulation of open-circuit voltage  $V_{OC}$  as a function of cell temperature.

The average accuracy is 5.197 % (Fig. 18).

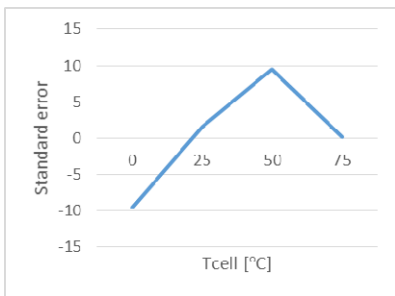


**Fig. 18.** Accuracy of simulation of the dependence of open-circuit voltage  $V_{OC}$  versus cell temperature; average accuracy: 5.197 %.

#### 4. CONCLUSION

The presented behavioral model of the ET-P660230WW 230W polycrystalline solar cell is open-coded in Matlab enabling its cross-platform usability. Simulation results demonstrate the validity of the model as they are within the manufacturer provided tolerances. Moreover, the fact that we simulate a state-of-the-art product available on the market prove the applicability of the model to real design tasks.

The model very well predicts the behavior of the solar cell in real environmental conditions. The simulation results accurately match the experiment: the accuracy of the short circuit current and open circuit voltage is under 4 %.

#### ACKNOWLEDGEMENTS

This work was supported by National Ministry of Science and Education of Bulgaria under Contract

DFNI-I01/9-3 “Information-measurement system for thermographic evaluation of potential failures and life protection of high reliability energy conversion elements”.

#### REFERENCES

- [1] G. Yu, J. Gao, J. C. Hummelen, F. Wudl, and A. J. Heeger, Science 270, 1995, p. 1789.
- [2] S. E. Shaheen, C. J. Brabec, F. Padinger, T. Fromherz, J. C. Hummelen, and N. S. Sariciftci, Appl. Phys. Lett. 78, 2001, p. 841.
- [3] M. Granström, K. Petritsch, A. C. Arias, A. Lux, M. R. Andersson, and R. H. Friend, Nature 395, 1998, p. 257.
- [4] J. J. M. Halls, A. C. Arias, J. D. MacKenzie, W. Wu, M. Inbasekaran, E. P. Woo, and R. H. Friend, Adv. Mater. 12, 2000, p. 498.
- [5] N. S. Sariciftci, L. Smilowitz, A. J. Heeger, and F. Wudl, Science 258, 1992, p. 1474.
- [6] ET-P660230WW Module Polycrystalline Data Sheet: <http://www.etsolar.com/upload/DownloadCenter/2012070301035914.pdf>.
- [7] L. Castaner, S. Silvestre, “Modelling Photovoltaic Systems using PSpice”, John Wiley and Sons, West Sussex, 2002.
- [8] R. Rusev, G. Angelov, I. Panayotov, T. Takov, M. Hristov, “Mathematical and Behavioral Modeling of Polycrystalline Solar Module”, Journ. of Advanced Materials and Operations (AMO) Society, Iss. 3, Vol. 1, 2010, pp. 43-46, ISSN 1313-8987.
- [9] G. Angelov, R. Rusev, E. Gieva, R. Radonov, T. Takov, M. Hristov, “Matlab Behavioral Model of Polymer-Fullerene Solar Cell”, Proc. of the 6<sup>th</sup> Colloque Francophone sur L’Energie - Environnement - Economie et Thermodynamique (COFRET’12), pp. 293-297, Sozopol, Bulgaria, June 11-13, 2012.